

Discrete chaotic states of a Bose-Einstein condensate

Wenhua Hai*, Shiguang Rong, Qianquan Zhu

*Key Laboratory of Low-dimensional Quantum Structures and Quantum Control of Ministry of Education, and Department of Physics, Hunan Normal University, Changsha 410081, China**

We find the different spatial chaos in a one-dimensional attractive Bose-Einstein condensate interacting with a Gaussian-like laser barrier and perturbed by a weak optical lattice. For the low laser barrier the chaotic regions of parameters are demonstrated and the chaotic and regular states are illustrated numerically. In the high barrier case, the bounded perturbed solutions which describe a set of discrete chaotic states are constructed for the discrete barrier heights and magic numbers of condensed atoms. The chaotic density profiles are exhibited numerically for the lowest quantum number, and the analytically bounded but numerically unbounded Gaussian-like configurations are confirmed. It is shown that the chaotic wave packets can be controlled experimentally by adjusting the laser barrier potential.

PACS numbers: 05.45.Ac, 05.45.Mt, 03.75.Hh, 05.30.Jp

I. INTRODUCTION

It is well-known that chaos in a nonlinear system not only may play a destructive role, but also has many practical and dramatic applications [1]. Chaos has been thoroughly studied during the last century in many different fields of physics. Very recently it has been recognized that existence of chaos is also possible in the Bose-Einstein condensates (BECs) described by the Gross-Pitaevskii equation (GPE) picture [2] and in the discretized systems describing trapped BECs within the space-mode approximation [3]. The temporal chaos was revealed in the time evolutions of BECs trapped in a double-well potential [4]. The spatial chaos with spatially disordered configurations was investigated for the stationary states of the BECs held in an optical lattice [5]. The spatiotemporal chaos in BECs interacting with different potentials has also been found [6].

The mean-field stationary states of a BEC are dominated by the time-independent one-dimensional (1D) GPE [7, 8]. For a BEC in ground state without current [7] the GPE is a real equation and can be identical with the celebrated Duffing equation [9, 10] by using time instead of spatial coordinate. Particularly, when such a GPE is perturbed by a weak periodic potential, the Smale-horseshoe chaos may appear for a certain parameter region of the extended dynamical system [9, 10]. The Melnikov chaos criterion gives the chaotic parameter region in which the perturbation parameters are allowed to vary their values continuously [11, 12, 13, 14]. The Gaussian-like barrier potentials can be realized by a sharply focused laser beam in the experiment [15], which have been applied to investigate the shock-wave formation in BECs [16], the nonlinear resonant transport [17]

and deterministic chaos [18] of BECs. Recently, using external fields to control quantum states of BECs has become an important physical motivation [19].

When a BEC is created initially in a time-independent optical lattice, the stationary states of the GPE are determined by the boundary conditions and are adjusted by the system parameters. The different boundary conditions may be established in a practical experiment, which cannot be set accurately. In the non-chaotic regimes, a small change of the boundary conditions and/or system parameters brings the BEC state only a small correction which can be neglected in a good approximation. In the chaotic regimes, however, the stationary state depends on the conditions and parameters sensitively. The sensitivity means that a small change of the conditions and/or parameters may cause a great difference which is not negligible. For example, the periodic configuration of BEC density is changed to the aperiodic and irregular one. It is important for the application purpose to predict the bounded states and to manipulate the corresponding density distributions which govern the beam profile of an atom laser extracted from the BEC [20]. Therefore, investigating the spatial chaos and its control is necessary and interesting for the considered BEC system.

The main aim of this paper is to present an analytical evidence of a different type of spatial chaos which can be defined as the discrete chaotic states, and to establish a method for controlling the chaotic states. By the discrete states we mean a denumerable set of bounded solutions in which any solution is one-to-one with a value in a discrete set of the parameter values. If the discrete states meet the Melnikov chaos criterion, we call them the discrete chaotic states. By using a laser beam modeled by the tanh-squared-shaped barrier potential [21] which is known as the Rosen-Morse potential [22], we demonstrate the existence of spatial chaos in the BEC held in a weak optical lattice. The chaotic regions of parameters are exhibited and the regular and disordered configurations of the BEC are illustrated. It is shown that the width and site of the strong barrier potential confine the width and site of the BEC wave-packet, and a denumer-

*Electronic address: whhai2005@yahoo.com.cn

able set of the barrier height values corresponds to the discrete chaotic states and magic numbers of condensed atoms. Thus the possible chaotic states can be controlled by adjusting the width, site and height of the laser barrier experimentally.

II. CHAOTIC AND REGULAR STATES FOR THE LOW LASER BARRIER

For the considered BEC system with transverse wave function being in ground state of a harmonic oscillator of frequency ω_r , the governing time-independent quasi-1D GPE reads

$$-\frac{\hbar^2}{2m}\psi_{xx} + [V'(x) + g'_{1d}|\psi|^2]\psi = \mu\psi, \quad (1)$$

where m is the atomic mass, μ is the chemical potential, and $g'_{1d} = g_0 m \omega_r / (2\pi\hbar) = 2\hbar\omega_r a_s$ denotes the quasi-1D atom-atom interaction intensity with a_s being the s -wave scattering length. Hereafter, by ψ_{xx} we mean the second derivative of ψ with respect to x . The external potential $V'(x) = -V_0 \tanh^2[\beta(x - x_c)] + V_1 \sin^2 kx$ contains the longitudinal barrier potential of strength $V_0 > 0$, width β^{-1} and center site x_c , and the perturbed lattice potential with V_1 and k being the intensity and wave vector. The former as a Gaussian-like potential can be formed by a sharply focused laser beam in the experiment [15], and the latter is a laser standing wave. Taking β^{-1} and β as the units of coordinate x and density $|\psi|^2$, and normalizing the potential strengths V_0, V_1 and chemical potential μ by using $E_\beta = \hbar^2\beta^2/m$, Eq. (1) becomes the dimensionless equation

$$-\frac{1}{2}\psi_{xx} + [V(x) + g_{1d}|\psi|^2]\psi = \mu\psi. \quad (2)$$

Here the interaction intensity is reduced to $g_{1d} = 2\hbar\omega_r a_s \beta / E_\beta = 2a_s / (\beta a_r^2)$ with $a_r = \sqrt{\hbar / (m\omega_r)}$ being the transverse harmonic oscillator length, and the potential gets the form

$$V(x) = -V_0 \tanh^2(x - x_c) + V_1 \sin^2 kx \quad (3)$$

with k measured in β .

We are interested in the real solution of GPE (2), which makes the GPE the perimetrically perturbed Duffing equation [10] in the spatial evolution and for the weak potential. It is well known that existence of the periodic perturbation is necessary for the appearance of chaos in the Duffing system [11, 12, 13]. When negative interaction and negative chemical potential are taken, in the absence of external potential the system has the well-known homoclinic (separatrix) solution [10, 11, 12, 13]

$$\begin{aligned} \psi_0 &= \sqrt{\frac{2\mu}{g_{1d}}} \operatorname{sech}[\sqrt{-2\mu}(x - c_0)], \\ C_0 &= \frac{1}{\sqrt{-2\mu}} \left\{ x_0 - \operatorname{Arc} \operatorname{sech} \left[\sqrt{\frac{g_{1d}}{2\mu}} \psi_0(x_0) \right] \right\}, \end{aligned} \quad (4)$$

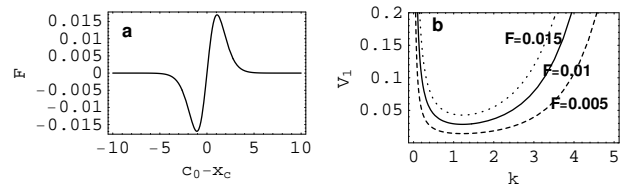


FIG. 1: (a) The constant F as a function of $c_0 - x_c$ for parameters $\mu = -2$ and $V_0 = 0.2$. (b) The boundaries of the chaotic regions for $\mu = -2$, and $F = 0.005$ (dashed curve), $F = 0.01$ (solid curve) and $F = 0.015$ (dotted curve).

where c_0 is an arbitrary constant adjusted by the boundary conditions at the boundary $x = x_0$. For the BEC system governed by Eq. (2) the constant c_0 cannot be determined experimentally, because of the undetectable $\psi_0(x_0)$. The presence of the weak external potential leads to the Melnikov function [10, 11, 12, 13]

$$\begin{aligned} M(c_0) &= \int_{-\infty}^{\infty} 2\psi_{0x}(x)V(x)\psi_0(x)dx \\ &= \frac{4\mu\sqrt{-2\mu}}{g_{1d}} \left[F - \frac{k^2\pi V_1 \sin(2kc_0)}{2\mu \sinh(k\pi/\sqrt{-2\mu})} \right] \end{aligned} \quad (5)$$

for $0 < V_0 \ll 1$ and $|V_1| \ll 1$, where ψ_{0x} denotes the first derivative of ψ_0 with respect to x , constant F from the barrier potential reads

$$F = \frac{4V_0 e^{2\Delta}}{|\mu|(e^{2\Delta} - 1)^4} [(3 + 2\Delta + 8\Delta e^{2\Delta} + (2\Delta - 3)e^{4\Delta})] \quad (6)$$

with $\Delta = c_0 - x_c$. The Melnikov function measures the distance between the stable and unstable manifolds in the Poincaré section of the equivalent phase space (ψ, ψ_x) . For some c_0 values if the Melnikov function has a simple zero, the locally stable and unstable manifolds intersect transversally such that the Smale-horseshoe chaos exists in the Poincaré map [10, 11, 12, 13]. The possibility of $M(c_0) = 0$ results in the chaotic region of parameter space

$$|V_1| \geq 2 \frac{|F\mu|}{\pi k^2} \sinh\left(\frac{k\pi}{\sqrt{-2\mu}}\right). \quad (7)$$

When parameters are taken in the chaotic region, the Melnikov function has zero points and the stable and unstable manifolds in the Poincaré section may intersect that leads to the Smale-horseshoe chaos. It is possible that the regular orbits exist for both the chaotic and non-chaotic regions. The chaotic and regular orbits in the chaotic region depend on the different boundary conditions respectively.

As can be seen from Eq. (7), for any negative chemical potential $\mu < 0$ and any barrier potential strength in the region $0 < V_0 \ll 1$, the chaotic region depends on constant F in the plane of parameters V_1 versus k . The F is determined by the parameters V_0, μ and $c_0 - x_c$ with the potential strength V_0 and site x_c being adjustable.

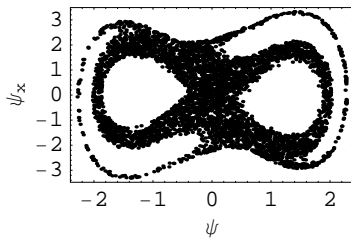


FIG. 2: The Poincaré section on the equivalent phase space (ψ, ψ_x) from Eq. (2) for the given parameters and boundary condition.

In Fig. 1a we show F as a function of $c_0 - x_c$ for $\mu = -2$ and $V_0 = 0.2$ by using the MATHEMATICA code. From this figure it can be observed that $|F|$ has a maximum $|F| = 0.015$ and a minimum $|F| = 0$. The former corresponds to the minimal chaotic region of Eq. (7), and the latter is associated with the maximal chaotic region $|V_1| > 0$. Taking $\mu = -2$ and $F = 0.005, 0.01, 0.015$ associated with three different c_0 values respectively, from Eq. (7) we plot the boundary curves of the chaotic regions as the dashed curve, solid curve and dotted curve of Fig. 1b. The corresponding chaotic regions are above these curves respectively. The minimal chaotic region above the curve of $|F| = 0.015$ is certainly chaotic region for arbitrary c_0 value. But the other chaotic regions are related to the corresponding boundary conditions, through the constant $F(c_0)$.

A useful way of analyzing chaotic motion is to look at what is called the Poincaré section, which is a discrete set of the phase space points at every period of the periodic potential, i.e. at $x = 2\pi/k, 4\pi/k, 6\pi/k, \dots$. Taking the parameters $\mu = -2, g_{1d} = -1, V_0 = 0.2, V_1 = 0.2, k = 1.5, x_c = 1$ and the approximation $[\psi(x_0), \psi_x(x_0)] = [\psi(10000), \psi_x(10000)] = (0.00001, 0.00001)$ to the experimentally possible boundary condition $[\psi(\infty), \psi_x(\infty)] = (0, 0)$, from Eq. (2) we numerically plot the Poincaré section on the equivalent phase space (ψ, ψ_x) and find the chaotic trajectory as in Fig. 2. Here the lattice strength V_1 and wave vector k are evaluated in the minimal chaotic region of Fig. 1b. For the same parameters of Fig. 2 from Eqs. (2) and (3) the potential and chaotic state functions are plotted as in Figs. 3a and 3b respectively. From Fig. 3a we can see the profile of the combined potential between the barrier potential and periodic lattice. In Fig. 3b we exhibit the aperiodicity and irregularity of the chaotic macroscopic wave function corresponding to Fig. 2 numerically. In order to confirm the sensitive dependence of chaotic system on the boundary conditions, we change only the boundary condition as $[\psi(10000), \psi_x(10000)] = (0, 0.00001)$ to plot the wave function. This small change leads the irregular curve in Fig. 3b to the periodic one in Fig. 3c. When the lattice strength is decreased to $V_1 = 0.005$ and the other parameters are kept, from Fig. 1b we observe that the parameter value is outside the given chaotic region. After changing V_1 from 0.2 to 0.005, Figs. 3a, 3b and

3c are changed to Figs. 4a, 4b and 4c respectively. Figure 4a displays the weak periodic potential compared to the laser barrier. In Fig. 4b and 4c we illustrate that in the considered parameter region the wave functions are periodic for the given boundary conditions. It is interesting noting that the regular wave functions in Figs. 4b have two different periods and two different amplitudes in both sides of the laser barrier. This means that the atomic number $\int_{\Sigma} |\psi(x)|^2 dx$ is different for the integration region Σ of different side. The periodicity is varied with the change of the boundary conditions from $[\psi(10000), \psi_x(10000)] = (0.00001, 0.00001)$ of Fig. 4b to $[\psi(10000), \psi_x(10000)] = (0, 0.00001)$ of Fig. 4c. Differing from Fig. 4b, in Fig. 4c the period of wave function in both sides of barrier is the sameness and the smaller one of amplitudes is enlarged compared to that of Fig. 4b. The results display the different profiles of macroscopic quantum states and reveal that the existence of chaos means the sensitive dependence of the BEC system on the boundary conditions and parameters.

III. DISCRETE CHAOTIC STATES FOR THE HIGH LASER BARRIER

The chaotic region of Eq. (7) is based on the perturbation theory [11, 12] so that it is valid only for very small potential strengths V_0 and V_1 . When the strength V_0 of the barrier potential is continuously increased to strong enough, e.g. $V_0 > 1$, it can no longer be treated as a part of perturbations. In this case we require to reconsider the perturbation problem of the stationary states. Applying the well-known Rayleigh-Schrödinger expansions [23]

$$\psi = \psi_0 + \psi_1, \quad \mu = \mu_0 + \mu_1 \quad \text{for } |\psi_1|, |\mu_1|, |V_1| \ll 1 \quad (8)$$

to Eq. (2) of real ψ , we have the leading order and the first order equations as

$$\begin{aligned} -\frac{1}{2}\psi_{0xx} - [V_0 \tanh^2(x - x_c) - g_{1d}\psi_0^2]\psi_0 &= \mu_0\psi_0, \quad (9) \\ -\frac{1}{2}\psi_{1xx} - [V_0 \tanh^2(x - x_c) - 3g_{1d}\psi_0^2 + \mu_0]\psi_1 \\ &= (\mu_1 - V_1 \sin^2 kx)\psi_0(x). \end{aligned} \quad (10)$$

Noticing that Eq. (9) has many special solutions for the fixed values of V_0, g_{1d}, x_c and different μ_0 values. Only the homoclinic solution is related to the Melnikov's chaos and the other solutions are associated with the regular states of Eq. (2). Here we are interested in the chaos and only consider the homoclinic solution thereby. It can be easily proved that the homoclinic solution of Eq. (9) has the form

$$\psi_0 = \sqrt{\frac{V_0 + 1}{-g_{1d}}} \text{sech}(x - x_c) \quad \text{for } \mu_0 = -V_0 - \frac{1}{2}. \quad (11)$$

Differing from Eq. (4), Eq. (11) describes a wave packet whose height and width are adjusted by the potential

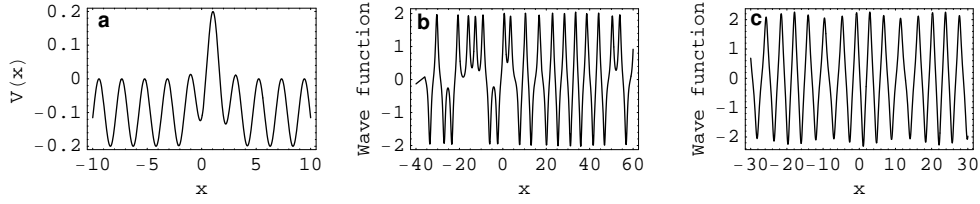


FIG. 3: (a) The potential function of Eq. (3) and (b) the aperiodic chaotic state of Eq. (2) for the same parameters and boundary condition with Fig. 2. (c) When the value of $\psi(10000)$ is changed from 0.00001 to 0, we get the periodic wave function.

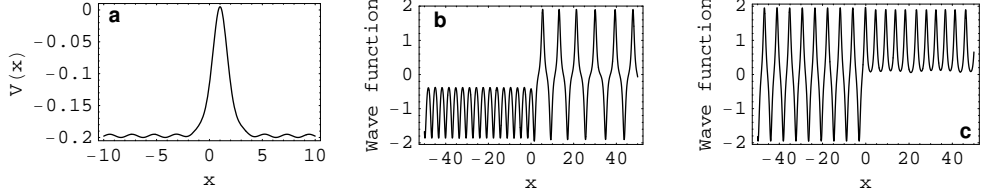


FIG. 4: The correspondences of Fig. 3 after the change of parameter V_1 from 0.2 to 0.005.

intensity V_0 and width β^{-1} implied in the unit of x . Substituting Eq. (11) into Eq. (10) yields the non-homogeneous equation

$$\begin{aligned} -\frac{1}{2}\psi_{1xx} - \left[(2V_0 + 3)\text{sech}^2(x - x_c) - \frac{1}{2} \right] \psi_1 \\ = -f(x) = (\mu_1 - V_1 \sin^2 kx)\psi_0(x). \end{aligned} \quad (12)$$

The corresponding homogeneous equation for $f = 0$ is a well-known Schrödinger one with trapping potential $-(2V_0 + 3)\text{sech}^2(x - x_c)$ and eigenenergy $E = -1/2$. Given two linearly independent solutions of the homogeneous equation as ψ'_1 and $\psi''_1 = \psi'_1 \int (\psi'_1)^{-2} dx$, the exact general solution of non-homogeneous Eq. (12) can be written in the integral form [24]

$$\psi_1 = 2\psi''_1 \int_A^x \psi'_1 f(x) dx - 2\psi'_1 \int_B^x \psi''_1 f(x) dx, \quad (13)$$

where A and B are arbitrary constants determined by the boundary and normalization conditions. This solution can be directly proved by comparing the second derivative ψ_{1xx} from Eq. (13) with that in Eq. (12).

Boundedness of the perturbed correction ψ_1 is the physical requirement, which depends on the bounded ψ'_1 . In order to seek such a ψ'_1 , we set [23]

$$\begin{aligned} \psi'_1 &= [\text{sech}(x - x_c)]^{2\lambda} u(z), \quad z = -\sinh^2(x - x_c), \\ \lambda &= [\sqrt{8(2V_0 + 3) + 1} - 1]/4. \end{aligned} \quad (14)$$

Inserting Eq. (14) into the homogeneous part of Eq. (12) with $f = 0$ produces the hypergeometric equation

$$z(1-z)u_{zz} + [0.5 - (a+b+1)z]u_z - abu = 0, \quad (15)$$

where $a = 0.5 - \lambda$, $b = -0.5 - \lambda$. Its two linear independent solutions with finite terms read [23]

$$\begin{aligned} u_n^e &= F(0.5 - \lambda, -0.5 - \lambda, 0.5, z) \quad \text{for } \lambda = 0.5 + n; \\ u_n^o &= \sqrt{|z|} F(1 - \lambda, -\lambda, 1.5, z) \quad \text{for } \lambda = 1 + n. \end{aligned} \quad (16)$$

Here $F(a, b, c, z)$ is the hypergeometric function, u_n^e and u_n^o with $n = 0, 1, 2, \dots$ denote even and odd functions of $(x - x_c)$ respectively. Combining Eq. (16) with Eq. (14) we arrive at the bounded solutions

$$\begin{aligned} \psi_{1n}^e &= [\text{sech}(x - x_c)]^{1+2n} u_n^e, \quad V_0 = [(3 + 4n)^2 - 25]/16, \\ \psi_{1n}^o &= [\text{sech}(x - x_c)]^{2+2n} u_n^o, \quad V_0 = [(5 + 4n)^2 - 25]/16 \\ &\quad \text{for } V_0 > 0, \quad n = 1, 2, \dots \end{aligned} \quad (17)$$

Noting that ψ'_1 of Eq. (17) tends to zero, and $\psi''_1 = \psi'_1 \int (\psi'_1)^{-2} dx$ of Eq. (13) is infinity at $x = \pm\infty$. Thus the second term of Eq. (13) is in the form of zero multiplying infinity at $x = \pm\infty$, so we can use the l'Hospital rule to calculate the limit and to prove the boundedness of this term. For the first term of Eq. (13) we have to establish the boundedness condition

$$I_{\pm} = \lim_{x \rightarrow \pm\infty} \int_A^x \psi'_1 (V_1 \sin^2 kx - \mu_1) \psi_0 dx = 0. \quad (18)$$

The necessity of Eq. (18) is obvious for the boundedness of Eq. (13), because of the unboundedness of ψ''_1 . Under condition (18) we can apply the l'Hôpital rule to the both terms of Eq. (13), obtaining [24] $\lim_{x \rightarrow \pm\infty} \psi_1 = 2 \lim_{x \rightarrow \pm\infty} f(x) = 0$. This limit implies that Eq. (18) is also sufficient and the obtained macroscopic wave function satisfies the usual boundary condition $\psi(\pm\infty) = \psi_0(\pm\infty) + \psi_1(\pm\infty) = 0$. Noticing the correspondence between $f(x)$ and $\varepsilon_k^{(1)}(x)$ in Eq. (9) of the second article of Ref. [24], the above proof of sufficiency is clear.

The integration of the first term in Eq. (13) is insolvable and cannot be expressed by finite elementary functions. Hence, in the numerical computation based on Eq. (13), small deviation from the exact value of the integration satisfying condition (18) is avoidable. The small deviation will be amplified exponentially fast by

the unbounded function $\psi_1''(x)$ until infinity as $x \rightarrow \pm\infty$ that exhibits the numerical instability. The analytical insolvability and numerical instability can cause the unpredictable chaotic behavior [14]. The difference $I_+ - I_-$ of the integration in Eq. (18) is similar to the Melnikov function of Eq. (5), hence $I_+ - I_- = 0$ can be called the generalized Melnikov criterion for chaos. In fact, given Eq. (18), the undetermined form $\psi_1''(\pm\infty) \times I_{\pm} = \infty \times 0$ appears in Eq. (13) as $|x|$ tending to infinity, which leads to a new feature as the analytical boundedness but numerical unboundedness, namely the evidenced incompatibility and unpredictability of the chaotic behavior [14]. Therefore, under the condition (18) the solution $\psi(x) = \psi_0(x) + \psi_1(x)$ in terms of Eqs. (11) and (13) is called the chaotic solution [14]. If the zero boundary condition $[\psi(\pm\infty), \psi_x(\pm\infty)] = (0, 0)$ is required theoretically, the uniqueness theorem infers the chaotic solution to be the unique one of the system. On the other hand, from the formula of the energy functional [7, 8],

$$\begin{aligned} H &= \int \psi^+ \left[-\frac{1}{2}\nabla^2 + V(\vec{r}) + \frac{1}{2}g_{1d}|\psi|^2 \right] \psi d^3x \\ &= \int \left[\frac{1}{2}|\nabla\psi|^2 + V(\vec{r})|\psi|^2 + \frac{1}{2}g_{1d}|\psi|^4 \right] d^3x \\ &\quad - \frac{1}{2}(\psi^+ \nabla\psi)|_{-\infty}^{\infty}, \end{aligned} \quad (19)$$

we know that unlike the unbounded solution with $|\psi^+(\pm\infty)| = \infty$, the analytically bounded solution with $\psi^+(\pm\infty) = 0$ is associated with the finite energy functional and may be metastable thereby [7]. Although the chaotic solution is not very stable, due to the sensitive dependence on the parameters and boundary conditions, it may also be metastable compared to the analytically unbounded solution. *Particularly, these bounded solutions are valid only for the discrete V_0 values of Eq. (17). This means the corresponding analytically bounded chaotic states to be discrete with the increase of the barrier height.*

The above-mentioned results imply that when the barrier potential is strong enough, its strength values must be discrete for the bounded perturbed solutions. For the discrete $V_0 = V_{0n}$ values the leading number-density ψ_0^2 is proportional to V_{0n} and the leading chemical potential is given as $\mu_{0n} = -\frac{1}{2} - V_{0n}$ by Eq. (11), the both are also discrete. The parameters V_1, k, x_c and g_{1d} can vary their values continually in a certain parameter regions. Given a set of values of V_1, k, x_c , the first correction μ_1 is determined by the boundedness condition of Eq. (18). In Eq. (10) the discrete chemical potential $\mu \approx \mu_{0n} + \mu_1$ is equivalent to the energy of a Schrödinger system. In quantum mechanics [23], it is known that the boundedness of wave function may lead the energy to take discrete values. Mathematically, the relationship between the discrete values of potential strength $V_0 = V_{0n}$ and the exactly bounded solutions of Eq. (12) agrees qualitatively with that of a 2D Coulomb correlated system [26], where the Schrödinger equation is exactly solvable only for a denumerably infinite set of values of magnetic strength (or

the corresponding oscillator frequency). Physically, we well know that for a 2D electron gas in a semiconductor heterojunction the integral and fractional quantum Hall plateaus are associated with the discrete set of values of magnetic strength [27].

We now investigate the physical effect of the discrete laser strength $V_0 = V_{0n}$ on the considered BEC system. Applying Eq. (11) to the normalization condition yields the number of condensed atoms $N_n \approx \int |\psi_{0n}|^2 dx = 2(1 + V_{0n})/|g_{1d}| = (1 + V_{0n})\beta a_r^2/|a_s|$ for the metastable states given by Eq. (8) with Eqs. (11) and (17), that results in the relation

$$N_n|a_s| \approx (1 + V_{0n})\beta a_r^2 \quad (20)$$

with V_{0n} given in Eq. (17). Here the special value N_n can be called the magic numbers of the macroscopic many-body system keeping in the metastable states. Differing from the magic numbers of the microscopic many-body system (e.g. atomic nucleus), N_n denotes some approximate values, because of the approximation $N \pm 1 \approx N$ in the mean-field theory of macroscopic many-body system [7, 8]. For a harmonically confined BEC system, the supercritical number N_{cr} of condensed atoms obeys [7] $N_{cr}|a_s| = 0.575a_{ho}$ with a_{ho} being the 3D harmonic oscillator length. The magic number N_n may exceed the supercritical number N_{cr} by increasing the laser strength V_{0n} and/or decreasing the laser barrier width β^{-1} . The approximate magic numbers of the considered many-body system warrants experimental investigation.

Let us take the simplest even solution of $(x - x_c)$ with quantum number $n = 1$ as an example to show the feature of the chaotic solutions. From Eqs. (17) and (16) such a solution is derived as

$$\psi'_{1n} = \psi'_{11} = \text{sech}^3 y (1 - 4 \sinh^2 y) \quad (21)$$

for $y = x - x_c$ and $V_{01} = 3/2$, $\mu_{01} = -1/2 - V_{01} = -2$. Obviously, this solution tends to zero as $x \rightarrow \pm\infty$. The corresponding unbounded solution reads

$$\begin{aligned} \psi''_{1n} &= \psi''_{11} = \psi'_{11} \int (\psi'_{11})^{-2} dx \\ &= \frac{1}{64} \text{sech}^3 y (36y - 24y \cosh 2y + 28 \sinh 2y - \sinh 4y) \end{aligned} \quad (22)$$

in which the term $\frac{1}{64} \text{sech}^3 y \sinh 4y$ tends to $\pm\infty$ and the other terms tend to zero as $x \rightarrow \pm\infty$. Applying Eqs. (21) and (22) to Eq. (13), the exact general solution of Eq. (12) becomes

$$\psi_{11}^e = 2\psi''_{11} \int_A^x \psi'_{11} f(x) dx - 2\psi'_{11} \int_B^x \psi''_{11} f(x) dx, \quad (23)$$

where $f(x) = -(\mu_1 - V_1 \sin^2 kx)\psi_0(x)$ is equal to zero at $x = \pm\infty$, because of $\psi_0(\pm\infty) = 0$. Applying the l'Hôpital rule to Eq. (23), we easily verify its boundedness [24], through the limit $\lim_{x \rightarrow \pm\infty} \psi_{11}^e(x) = 0$ for the

μ_1 obeying Eq. (18) accurately. Inserting ψ_{11}^e and Eq. (11) into Eq. (18), from the generalized Melnikov chaos criterion $I_+ - I_- = 0$ one derives

$$\mu_1 = 0.5\pi V_1 \cos(2kx_c)k(5k^2 - 1)\text{csch}(k\pi) \quad (24)$$

which can be adjusted by the laser site x_c and has a maximum and a minimum at $\cos(2kx_c) = \pm 1$ respectively.

In order to obtain the bounded numerical solution of Eq. (23), the parameter μ_1 must obey Eq. (24). However, in any numerical computation, for a set of fixed parameters V_1, k, x_c it is impossible to take the value of μ_1 accurately, because of the irrational π with infinite sequence of digits in Eq. (24). This implies small deviation from the accurate boundedness condition (18) and the small deviation will lead the numerical solution of Eq. (23) to be exponentially amplified by the unbounded function ψ_{11}^e until infinity as $x \rightarrow \pm\infty$. So the analytically bounded chaotic solution (23) is numerically unbounded and uncomputable for sufficiently large $|x|$ values [14]. For a small $|x|$ value ψ_{11}^e is finite and Eq. (23) is certainly bounded. At $x = \pm\infty$ the boundedness condition (18) and l'Hôpital rule lead Eq. (23) to zero analytically. The unpredictability of chaotic solution (23) may occur only near the spatial range $|y| = |x - x_c| \in (|y_s|, \infty)$, where $y_s = x_s - x_c$ can be estimated through the starting point of the numerical incomputability after which the solution tends to infinity rapidly. In such a spatial range, the chaotic region of atomic density may be $|\psi(y)|^2 \in (2|\psi_0(\pm\infty)\psi_{11}^e(\pm\infty)|, 2|\psi_0(y_s)\psi_{11}^e(y_s)|) = (0, 2|\psi_0(y_s)\psi_{11}^e(y_s)|)$ with width $\delta(y)$ tending to zero as the increase of $|y|$ value. The maximal width reads $\delta(y_s) \approx 2|\psi_0(y_s)\psi_{11}^e(y_s)|$ which is in order of perturbation V_1 , since $|\psi(y)|^2$ equates $|\psi_0(y) + \psi_{11}^e(y)|^2 \approx |\psi_0(y)|^2 + 2|\psi_0(y)\psi_{11}^e(y)|$ and $|\psi_0(y)|^2$ is predictable for any y . The effective first-order correction to the Gaussian-like profile is analytical bounded, which can be obtained by cutting the infinity from the numerical solution of Eq. (23). These will be illustrated numerically as follows.

As an instance, setting the parameters $V_0 = V_{01} = 3/2, V_1 = 0.05, k = 1.5, g_{1d} = -1, \mu_0 = -2$ and the boundary condition which is equivalent to $A = -\infty, B = 0$, from Eqs. (11) and (23) we plot the chaotic atomic density $|\psi|^2 = (\psi_0 + \psi_{11}^e)^2$ as in Fig. 5a. Here the solid and dashed curves correspond to $x_c = 1, \mu_1 = -0.02148$ and $x_c = 2, \mu_1 = 0.02083$ respectively, which satisfy the generalized Melnikov chaos criterion (18) and (24) approximately. The dashed curve has approximate shape with the solid one and can be regarded as the latter after a translation of distance 1. The numerically unbounded first corrections are uncomputable for sufficiently large $|y| = |x - x_c|$ values and the starting points of the incomputability are shown to be about $y = \pm y_s \approx \pm 2$ after which the atomic densities may be irregular and tend to infinity rapidly. By using the wide-black curves instead of the infinity in range $|x - x_c| \geq 2$ of Fig. 5a, we obtain the Gaussian-like wave packets as in Fig. 5b which describe the analytically bounded atomic density better. The wide-black parts are the sketch maps of the chaotic

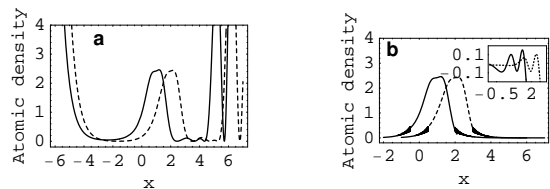


FIG. 5: (a) The chaotic density profiles of atomic number for $x_c = 1$ (solid curve) and $x_c = 2$ (dashed curve). (b) The analytically bounded density profiles from Fig. 5a by replacing the parts of $|x - x_c| > 2$ with the sketch maps of the chaotic density regions.

regions of density distributions, whose width varies from the maximal value $\delta(y_s) \sim V_1$ to minimal one $\delta(\pm\infty) = 0$. In the chaotic regions of density, the atomic density is unpredictable. The effective first corrections in the range $x \in (-0.5, 3)$ are exhibited by the inset of Fig. 5b, which are plotted from Eq. (23) for the range $|y| < 2$ and the parameters adopted in Fig. 5a. It should be emphasized that the analytically bounded chaotic states are discrete and can be manipulated experimentally by taking the barrier heights V_{0n} in Eq. (17) discontinuously and adjusting the barrier site x_c continuously. Particularly, by increasing x_c adiabatically [28], we can move the Gaussian-like wave packets slowly for the purpose of BEC transport [17].

IV. CONCLUSIONS AND DISCUSSIONS

We have investigated the spatial structure of the 1D attractive BEC interacting with a tanh-squared-shaped laser barrier potential and perturbed by a weak laser standing wave. The existence of the Smale-horseshoe chaos is demonstrated and the Melnikov chaotic regions of parameter space are displayed. In the low laser barrier case, the aperiodic chaotic states and periodic regular states are illustrated numerically. For the sufficiently strong barrier potential a set of discrete chaotic solutions is constructed formally. Any chaotic solution is the combination of a Gaussian-like wave-packet with the corresponding perturbed correction. The discrete chaotic solutions are analytically bounded only for the discrete barrier height values and special magic numbers of condensed atoms. The density profiles of BEC in the discrete chaotic states are investigated numerically for the lowest quantum number, and the numerical instability is revealed. The Gaussian-like wave could be translated by varying the laser-barrier site adiabatically, which is similar to the bright soliton of an attractive BEC with the parabolic barrier potential [25]. The periodic structures of BEC can be detected by the Bragg scattering of an optical probe beam [29] and the used Gaussian-like potential can be generated by a sharply focused laser beam in the experiments [15]. Thus the irregular chaotic states could be observed and controlled readily with current ex-

perimental capability.

The existence of chaos means the sensitive dependence of the BEC system on the boundary conditions and parameters in chaotic region. The sensitivity causes the unpredictability of the spatial distributions of the BEC atoms, since the boundary conditions cannot be set accurately in a real experiment. The above results reveal the possible bounded states associated with the spatial distributions, and suggest a method to control the irregular chaotic states by adjusting the lattice strength and laser barrier parameters.

It is worth noting that the discrete chaotic states may

appear in many different physical systems with different Gaussian-like potentials and may also exist in the temporal and spatiotemporal evolutions of the time-dependent systems.

Acknowledgments

This work was supported by the National Natural Science Foundation of China under Grant Nos. 10575034 and 10875039.

-
- [1] J. H. Kim and J. Stringer, *Applied Chaos* (John Wiley and Sons, Inc. New York, 1992).
- [2] Q. Thommen, J. C. Garreau, and V. Zehle, *Phys. Rev. Lett.* **91**, 210405(2003); C. Zhang, J. Liu, M.G. Raizen, and Q. Niu, *ibid.* **93**, 074101(2004); J. Liu, C. Zhang, M.G. Raizen, and Q. Niu, *Phys. Rev. A* **73**, 013601(2006); L. Salasnich, *Phys. Lett. A* **266**, 187(2000); W. Hai, C. Lee and Q. Zhu, *J. Phys. B: At. Mol. Opt. Phys.* **41**, 095301(2008).
- [3] P. Buonsante, R. Franzosi, and V. Penna, *Phys. Rev. Lett.* **90**, 050404(2003); G. P. Berman, F. Borgonovi, F.M. Izrailev, and A. Smerzi, *ibid.* **92**, 030404(2004); A. R. Kolovsky, *ibid.* **99**, 020401(2007); C. L. Pando L. and E. J. Doedel, *Phys. Rev. E* **75**, 016213 (2007).
- [4] F. Kh. Abdullaev and R. A. Kraenkel, *Phys. Rev. A* **62**, 023613(2000); C. Lee, W. Hai, L. Shi, X. Zhu and K. Gao, *Phys. Rev. A* **64**, 053604(2001).
- [5] V.M. Eguiluz, E. Hernandez-Garcia, O. Piro and S. Balle, *Phys. Rev. E* **60**, 6571(1999); G. Chong, W. Hai, Q. Xie, *Chaos* **14**, 217(2004); *Phys. Rev. E* **71**, 016202(2005).
- [6] G. Chong, W. Hai and Q. Xie, *Phys. Rev. E* **70**, 036213(2004); A. D. Martin, C. S. Adams, and S. A. Gardiner, *Phys. Rev. Lett.* **98**, 020402(2007); F. Li, W.X. Shu, J.G. Jiang, H.L. Luo, and Z. Ren, *Eur. Phys. J. D* **41**, 355 (2007).
- [7] F. Dalfovo, S. Giorgini, L.P. Pitaevskii and S. Stringari, *Rev. Mod. Phys.* **71**, 463(1999).
- [8] A. J. Leggett, *Rev. Mod. Phys.* **73**, 307(2001).
- [9] J. Holmes, *Philos. Trans. Roy. Soc., London* **292**, 419(1979); F. Moon, *Phys. Rev. Lett.* **53**, 962(1984); A. Venkatesan, M. Lakshmanan, A. Prasad and R. Ramaswamy, *Phys. Rev. E* **61**, 3641(2000).
- [10] S. Parthasarathy, *Phys. Rev. A* **46**, 2147(1992).
- [11] V. K. Melnikov, *Trans. Mosc. Math. Soc.* **12**, 1 (1963).
- [12] Z. Liu, *Perturbation Criteria for Chaos* (Shanghai Scientific and Technological Education Press, Shanghai, 1994) (in Chinese).
- [13] J. Gukenheimer and P. Holmes, *Nonlinear Oscillations, Dynamical Systems, and Vector Fields* (Springer, New York, 1983).
- [14] W. Hai, C. Lee, G. Chong and L. Shi, *Phys. Rev. E* **66**, 026202(2002); W. Hai, Q. Xie, J. Fang, *Phys. Rev. A* **72**, 012116 (2005); W. Hai, X. Liu, J. Fang, X. Zhang, W. Huang, G. Chong, *Phys. Lett. A* **275**, 54 (2000).
- [15] S. Burger, K. Bongs, S. Dettmer, W. Ertmer, and K. Sengstock, A. Sanpera, G. V. Shlyapnikov, and M. Lewenstein, *Phys. Rev. Lett.* **83**, 5198 (1999); J. Denschlag, J. E. Simsarian, D. L. Feder, W. C. Clark, L. A. Collins, J. Cubizolles, L. Deng, E. W. Hagley, K. Helmerson, W. P. Reinhardt, S. L. Rolston, B. I. Schneider, and W. D. Phillips, *Science* **287**, 97 (2000).
- [16] T. P. Simula, P. Engels, I. Coddington, V. Schweikhard, E. A. Cornell, and R. J. Ballagh, *Phys. Rev. Lett.* **94**, 080404 (2005).
- [17] T. Paul, K. Richter, and P. Schlagheck, *Phys. Rev. Lett.* **94**, 020404 (2005).
- [18] P. Couillet and N. Vandenberghe, *Phys. Rev. E* **64**, 025202(R) (2001); X. Luo and W. Hai, *Chaos*, **15**, 033702 (2005); S.K. Adhikari, *J. Phys. B* **38**, 579(2005).
- [19] C. E. Creffield and T. S. Monteiro, *Phys. Rev. Lett.*, **96**, 210403(2006); A. Eckardt, C. Weiss, and M. Holthaus, *Phys. Rev. Lett.*, **95**, 260404(2005).
- [20] M. Köhll, Th. Busch, K. Mølmer, T. W. Hänsch, and T. Esslinger, *Phys. Rev. A* **72**, 063618(2005).
- [21] S. J. Wang, C. L. Jia, D. Zhao, H. G. Luo, J. H. An, *Phys. Rev. A* **68**, 015601(2003); C. Lee, J. Brand, *Europhys. Lett.*, **73**, 321(2006).
- [22] G.L. Lamb, *Elements of Soliton Theory* (Wiley, New York, 1980).
- [23] J. Zeng, *Quantum Mechanics* (Science Press, Beijing, 2000, Vol. I, p496; Vol. II, p498) (in Chinese).
- [24] W. Hai, M. Feng, X. Zhu, L. Shi, K. Gao and X. Fang, *Phys. Rev. A* **61**, 052105(2000); W. Hai, X. Zhu, M. Feng, L. Shi, K. Gao and X. Fang; *J. Phys. A* **34**, L79(2001).
- [25] L. Khaykovich, F. Schreck, G. Ferrari, T. Bourdel, J. Cubizolles, L. D. Carr, Y. Castin, and C. Salomon, *Science* **296**, 1290 (2002); Z. X. Liang, Z. D. Zhang, W. M. Liu, *Phys. Rev. Lett.* **94**, 050402 (2005).
- [26] M. Taut, *Phys. Rev. A* **48**, 3561(1993).
- [27] R.E. Prange and S. Givin, *The Quantum Hall Effect*, 2nd ed. (Springer Verlag, New York, 1990).
- [28] H. Pu, P. Maenner, W. Zhang, and H. Y. Ling, *Phys. Rev. Lett.*, **98**, 050406 (2007).
- [29] D.V. Strekalov, A. Turlapov, A. Kumarakrishnan and T. Sleator, *Phys. Rev. A* **66**, 023601(2002).